

A new electrical configuration for improving the range of piezoelectric bimorph benders



Shannon A. Rios*, Andrew J. Fleming

Precision Mechatronics Laboratory, School of Electrical Engineering and Computer Science, The University of Newcastle, Callaghan, NSW 2308, Australia

ARTICLE INFO

Article history:

Received 25 August 2014

Received in revised form 28 January 2015

Accepted 28 January 2015

Available online 7 February 2015

Keywords:

Piezoelectric actuators

Bimorph

Bender

ABSTRACT

This article describes a new electrical configuration for driving piezoelectric benders. The 'Biased Bipolar' configuration is compatible with parallel-poled, bimorph and multimorph benders. The new configuration is similar to the standard three-wire drive method where the top electrode is biased with a DC voltage and the bottom electrode is grounded. However, the new configuration uses an alternate DC bias voltage and adjusted range for the central electrode which allows the full range of positive and negative electric fields to be utilized. Using this technique, the predicted deflection and force can be increased by a factor of 2.2 compared to the standard two wire configuration and 1.3 times for the standard three wire configuration. These predictions were verified experimentally where the measured factor of improvement in displacement and force was of 2.4 and 1.3 compared to the standard two-wire and three-wire configurations.

Crown Copyright © 2015 Published by Elsevier B.V. All rights reserved.

1. Introduction

Piezoelectric actuators utilize the inverse piezoelectric effect, where an applied electric field can induce an internal stress. These actuators are already used in a wide range of applications such as ultrasonic motors [1], beam steering [2], vibration dampening [3] and miniature robotics [4]. Piezoelectric actuators have a high stiffness, resolution and fast response compared to other common actuators. The most common type of piezoelectric actuator in industrial applications is the bender.

Benders can be of the unimorph or bimorph type. Unimorph actuators have one piezoelectric plate bonded to a non-piezoelectric elastic plate. Bimorph actuators, shown in Fig. 1, have two piezoelectric plates joined together possibly with a third elastic layer sandwiched between the two piezoelectric layers to increase the mechanical reliability [5]. The beam or plate is usually mounted in a cantilever arrangement; however, it can also be simply supported or fixed on both ends. Bimorph and unimorph actuators develop deflection and force when one piezoelectric layer contracts while the other layer expands, or in the case of unimorphs only when the piezoelectric layer contracts or expands. An additional type of bender is the multi-layer bender. Multi-layer benders

work in a similar fashion to bimorph benders except that each piezoelectric plate is comprised of many thinner piezoelectric layers co-fired together, thus reducing the maximum driving voltages required.

This paper explores existing electrical configurations and compares them to a proposed method for driving bimorph and multilayer piezoelectric benders. The new driving method allows a bender to be driven using the full range of electric field with only a single bias supply and a single variable power supply. By using this configuration, the size of a piezoelectric bender can be reduced while maintaining the same deflection as a larger bender driven with an existing electrical configuration.

In the following section, the history of piezoelectric bimorph benders is briefly discussed. Section 3 then describes the constituent equations for the deflection and blocking force. The new configuration is then presented, followed by experimental results.

2. History

The first piezoelectric benders were invented by Sawyer in 1931. These early benders used Rochelle salt bars cut at specific angles and cemented together to create bimorph benders. These benders were used primarily for audio applications such as microphones, speakers and pick-ups [6]. In 1936, Sawyer patented the series and parallel configurations for driving a bimorph bender [7]. These configurations remained the only available methods for driving a bimorph or multi-morph bender until 1993 when Hayashi et al.

* Corresponding author. Tel.: +61 413072013.

E-mail addresses: shannon.rios@newcastle.edu.au (S.A. Rios), andrew.fleming@newcastle.edu.au (A.J. Fleming).

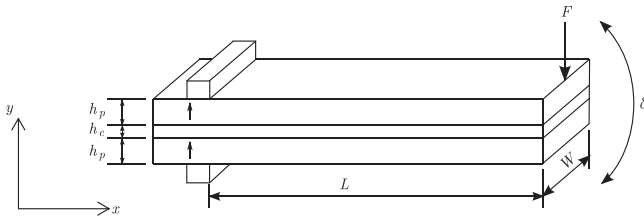


Fig. 1. Typical piezoelectric bimorph bender.

lodged US patent 5,233,256 outlining a new method for driving parallel and series configuration benders [8].

In 2005, Wood et al. proposed an electrical configuration for bimorphs that used one bias voltage and another unipolar voltage as part of their study on the optimal energy density of piezoelectric bending actuators [9]. This configuration was similar to US patent 5382864-A which switches the center electrode between the bias voltage and ground [10] and US patent 6888291-B2 which describes a method for driving an electrostrictive bimorph actuator by controlling the center voltage between the top and bottom electrode voltages [11].

In 1991, Smits et al. developed a set of constituent equations to describe the behavior of piezoelectric bimorphs for various mechanical boundary conditions including: a moment at the end of the beam, a force perpendicular to the beam applied at the tip and a uniformly distributed body load [12]. Following on from the work of Smits et al., Wang and Cross used similar techniques in 1999 to develop the constituent equations for symmetrical triple layer bimorph benders where the outer two layers are piezoelectric and the inner layer is a non-piezoelectric elastic layer [5].

Due to the advantageous properties of piezoelectric benders, they have recently found use in the field of miniature robotics [14,4,15]. Campolo et al. (2003) developed a unimorph actuator with an embedded piezoelectric sensor for use in a micro-mechanical flying insect [13]. A model for the sensor was developed and verified by experimentation. Piezoelectric benders are also used in industrial applications such as textile machines, fluid control devices and beam steering [16–18].

3. Bimorph model

A piezoelectric bender consists of two piezoelectric plates glued together, usually with a center shim laminated between the plates and mounted as a cantilever beam. The piezoelectric plates can either be polarized in the same direction or in opposite directions, this is referred to as the polling direction. By controlling the voltage across the piezoelectric plates with respect to the polling direction, the beam can be made to bend up or down and extend or contract.

In Fig. 1, a typical bimorph bender is illustrated with a center shim and a positive polarization direction indicated by the arrows. A positive voltage would be one that is higher at the tip compared to the base of the arrow. The maximum and minimum voltage, V_{\max} and V_{\min} respectively, that can be applied across each plate is derived from the poling and coercive electric field strength, E_p and E_c respectively, that is

$$V_{\max} = E_p h,$$

$$V_{\min} = E_c h.$$

The poling field is defined as the point at which an increase in electric field has little or no effect to the stress in the layer, usually around 1–2 kV/mm. The coercive field is the point at which the piezoelectric layer will start to depolarize, typically between –200 to –500 V/mm.

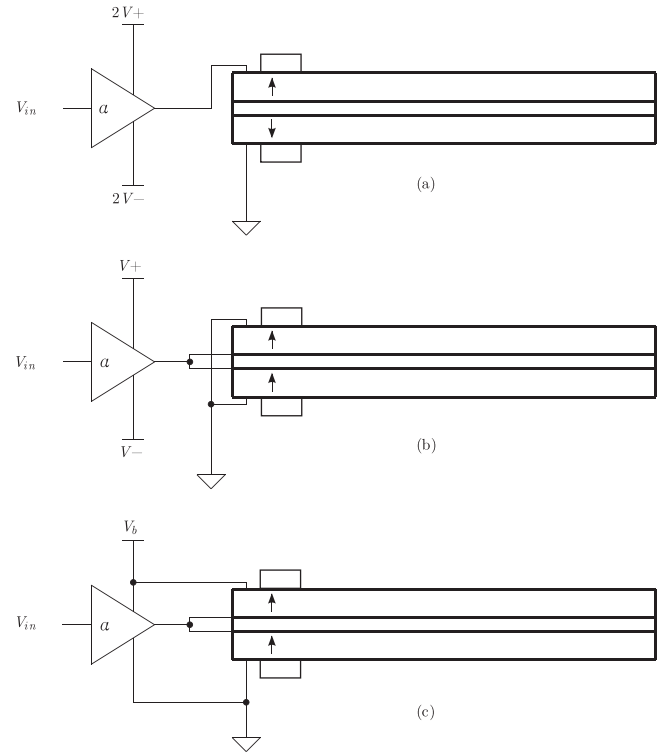


Fig. 2. Electrical configurations: (a) 'Series', (b) 'Parallel', (c) 'Biased Unipolar'.

The relationships between the tip deflection $\delta(x)$, blocking force $F_{blk}(x)$ and the applied voltages are,

$$\delta(x) = d_{31} Y_p h_m (V_A - V_B) \frac{x^2}{2D}, \quad (1)$$

$$F_{blk}(x) = d_{31} Y_p h_m (V_A - V_B) \frac{W}{x}, \quad (2)$$

where $\delta(x)$ is the tip deflection, d_{31} is the piezoelectric constant, Y_p is the Young's modulus of the piezoelectric material, h_m is the distance between the centroid of the piezoelectric layer and the neutral axis, V_A and V_B are the voltages applied across the top and bottom piezoelectric layers respectively, and D is the flexural stiffness of the beam. The derivation for these equations is reported in previous work [12,5,21].

4. Existing electrical configurations

The three most common electrical configurations for driving a piezoelectric bimorph bender are the 'Series', 'Parallel' and 'Biased Unipolar' configurations, which are illustrated in Fig. 2. This section will identify and compare the main features of each electrical configuration.

To more easily compare the performance of the different electrical configurations a baseline deflection and blocking force is defined such that δ_0 and F_0 is equal to the deflection and force produced by the parallel and series electrical configurations. Using this baseline a performance factor, γ can be defined as $\gamma = \delta/\delta_0 = F/F_0$. To further simplify the comparison, another factor, β , is defined to relate the maximum and minimum driving voltage, $V_{\max} = -\beta V_{\min}$. For example, if the specified maximum voltage is 200 V and the minimum voltage is –50 V, then $\beta = 4$.

For each of the following cases V_{in} is the control signal and is varied between [–1, 1]. The maximum deflection and force will occur at ± 1 V input to the system.

4.1. 'Series' configuration

The 'Series' configuration uses only two wires and the polling direction of the two layers are opposite. This method requires $V_{pp} = 4 |V_{\min}|$ where V_{pp} is the peak-to-peak voltage which is generated by a single amplifier. For the series bender seen in Fig. 2 the gain (α), extension (ϵ_x), tip deflection (δ), blocking force (F_{blk}) and capacitance (C) are

$$\alpha = |2V_{\min}|, \quad (3)$$

$$\gamma = 1, \quad (4)$$

$$\epsilon_x = 0, \quad (5)$$

$$\delta(L) = d_{31} Y_p h_m (2 |V_{\min}| V_{in}) \frac{L^2}{2D}, \quad (6)$$

$$F_{blk}(L) = d_{31} Y_p h_m (2 |V_{\min}| V_{in}) \frac{W}{L}, \quad (7)$$

$$C = \frac{K \epsilon_0 L W}{2h_p}. \quad (8)$$

4.2. 'Parallel' configuration

The 'Parallel' configuration is another two wire configuration where the polling direction of the two layers is aligned. One wire is connected to the center electrode and the other wire is connected to the two outer electrodes. Only one amplifier is required with a peak-to-peak voltage of $V_{pp} = 2 |V_{\min}|$. For the parallel bender seen in Fig. 2 the gain (α), extension (ϵ_x), tip deflection (δ), blocking force (F_{blk}) and capacitance (C) are

$$\alpha = |V_{\min}|, \quad (9)$$

$$\gamma = 1, \quad (10)$$

$$\epsilon_x = 0, \quad (11)$$

$$\delta(L) = d_{31} Y_p h_m (2 |V_{\min}| V_{in}) \frac{L^2}{2D}, \quad (12)$$

$$F_{blk}(L) = d_{31} Y_p h_m (2 |V_{\min}| V_{in}) \frac{W}{L}, \quad (13)$$

$$C = \frac{2K \epsilon_0 L W}{h_p}. \quad (14)$$

4.3. 'Biased Unipolar' configuration

The 'Biased Unipolar' configuration requires three wires and three electrodes to operate. Unlike the previous methods, two voltage supplies are required: one bias supply, $V_b = V_{\max}$, and the other controlled supply between 0V to V_{\max} . For the unipolar bender in Fig. 2 the gain (α), extension (ϵ_x), input offset voltage (V_o), tip deflection (δ), blocking force (F_{blk}) and capacitance (C) are

$$\alpha = \frac{V_{\max}}{2}, \quad (15)$$

$$\gamma = \frac{\beta}{2}, \quad (16)$$

$$V_o = 1 V, \quad (17)$$

$$\epsilon_x = \frac{d_{31} Y_p (V_{\max})}{(2h_p + h_c) Y_c}, \quad (18)$$

$$\delta(L) = d_{31} Y_p h_m (V_{\max} V_{in}) \frac{L^2}{2D}, \quad (19)$$

$$F_{blk}(L) = d_{31} Y_p h_m (V_{\max} V_{in}) \frac{W}{L}, \quad (20)$$

$$C = \frac{2K \epsilon_0 L W}{h_p}. \quad (21)$$

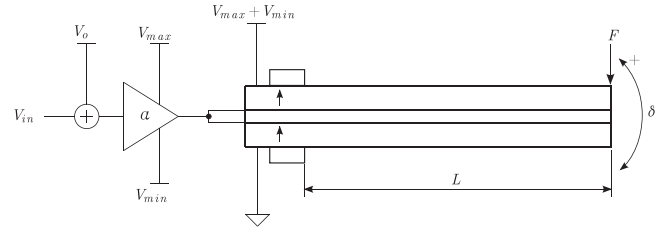


Fig. 3. 'Biased Bipolar' bender configuration.

5. 'Biased Bipolar' configuration

The 'Biased Bipolar' electrical configuration, shown in Fig. 3, is a new technique for driving three electrode, three wire, parallel poled piezoelectric benders, including bimorphs and multimorphs. This technique achieves greater deflection and force than previous configurations by using the full range of available positive and negative electric field. The voltage V_{in} in this example varies between $\pm 1 V$, however any input voltage could be used as long as the gain (α) and offset (V_o) are set accordingly.

For the bender seen in Fig. 3 the gain (α), offset voltage (V_o), extension (ϵ_x), tip deflection (δ), blocking force (F_{blk}) and capacitance (C) are,

$$\alpha = \frac{V_{\max} - V_{\min}}{2}, \quad (22)$$

$$\gamma = \frac{(\beta + 1)}{2}, \quad (23)$$

$$V_o = \frac{V_{\max} + V_{\min}}{V_{\max} - V_{\min}}, \quad (24)$$

$$\epsilon_x = \frac{d_{31} Y_p (V_{\max} + V_{\min})}{(2h_p + h_c) Y_c}, \quad (25)$$

$$\delta(L) = d_{31} Y_p h_m (V_{\max} - V_{\min}) V_{in} \frac{L^2}{2D}, \quad (26)$$

$$F_{blk}(L) = d_{31} Y_p h_m (V_{\max} - V_{\min}) V_{in} \frac{W}{L}, \quad (27)$$

$$C = \frac{2K \epsilon_0 L W}{h_p}. \quad (28)$$

By shifting the supply and bias voltages the 'Biased Bipolar' configuration can also be implemented with a symmetric power supply, shown in Fig. 4. This configuration is electrically identical to that seen in Fig. 3.

Compared to the 'Biased Unipolar' configuration, no additional power supplies are needed, and only a modest increase in peak to peak voltage is required. Similar to the 'Biased Unipolar' configuration, a voltage of $\frac{1}{2} (V_{\max} + V_{\min})$ is required to be present on the middle layer for 0 mm deflection, which is less than that required by the 'Biased Unipolar' configuration.

For a three wire multi-layer bender with the center electrode connected to the input signal, the top electrodes would alternate

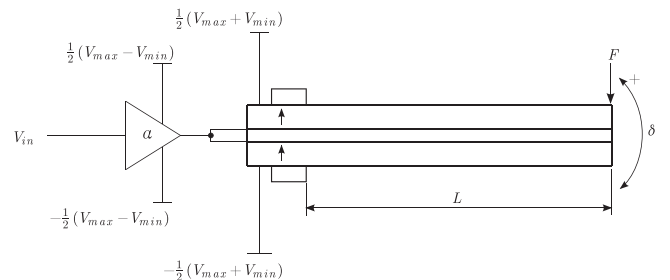


Fig. 4. 'Biased Bipolar' symmetric power supply rails configuration.

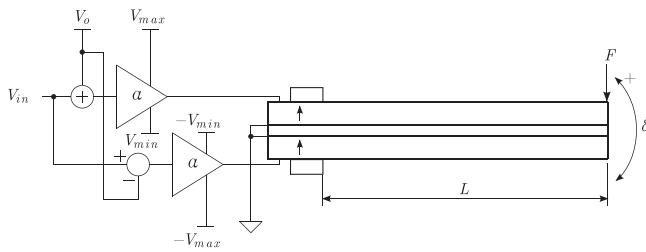


Fig. 5. 'Bridged Bipolar' parallel polled bender.

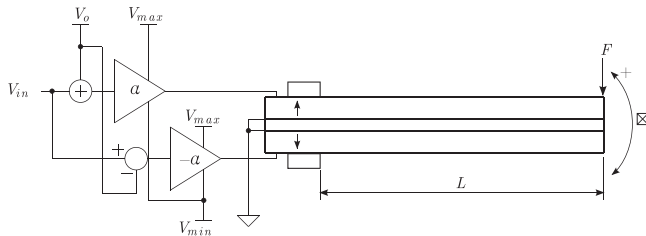


Fig. 6. 'Bridged Bipolar' series polled bender.

between the bias voltage and the control voltage, while the bottom half electrodes would alternate between the ground or negative bias voltage and the control voltage. By driving the bender using this method with a voltage ratio of $\beta = 3\frac{1}{3}$, the relative increase in deflection and force is $\gamma = 2.167$. This is a 30% increase when compared to the standard unipolar configuration.

6. 'Bridged Bi-polar' configuration

The 'Bridged Bipolar' configuration, seen in Figs. 5 and 6, requires two amplifiers per bender but may be a preferable configuration for benders with outward polarization since no bias supply is required. The 'Bridged Bipolar' configuration can be used on both aligned and opposite polled benders. One additional possibility of using the 'Bridged Bipolar' configuration is the ability to use the beam as an extender by changing the phase difference or voltage offset of the two power supplies. For the 'Bridged Bipolar' configuration seen in Figs. 5 and 6, the gain (α), extension (ϵ_x), input offset voltage (V_0), tip deflection (δ), blocking force (F_{blk}) and capacitance (C) are equivalent to the 'Biased Bipolar' electrical configuration described in Section 5.

7. Experimental results

An experiment was conducted to compare the bender control methods and assess the accuracy of the analytical model. The experiment was performed using a two layer, parallel polled piezoelectric plate from PIEZO SYSTEMS, Inc. The plate measured 31.8 mm \times 63.5 mm, was 0.51 mm thick and was constructed from PSI-5A4E type piezoceramic, a summary of the relevant material properties can be found in Table 1. The plate was mounted to a

Table 1
Piezoelectric material properties.

K	1800
d_{31}	3.9×10^{-10} m/V
L_{free}	57 mm
W	31.8 mm
h_p	0.2 mm
h_c	0.1 mm
Y_p	52 GPa
Y_c	110 GPa

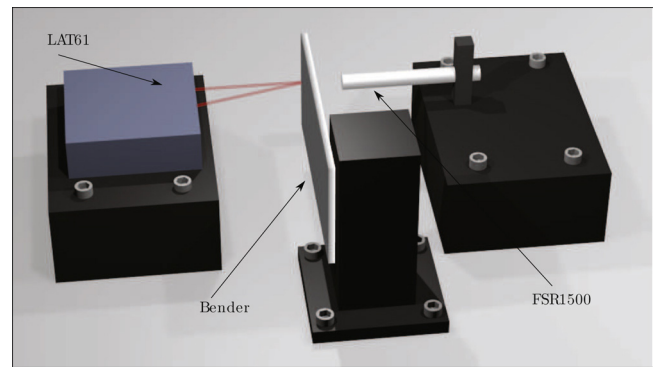


Fig. 7. Experimental setup.

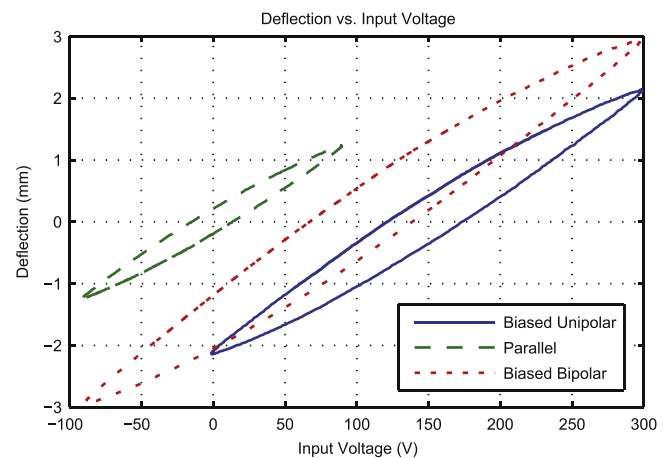


Fig. 8. Bender hysteresis.

board using epoxy such that the free length was 57 mm. This actuator has a V_{max} of 300 V and V_{min} of -90 V [19].

In order to accurately measure both the tip deflection and the blocking force, the experimental set up illustrated in Fig. 7 was developed. A Di-Soric LAT61 Laser distance sensor measured the displacement and a HONEYWELL FSS1500NS piezo-resistive sensor measured the force. The distance sensor has a 0–10 V output signal and the force sensor gives a differential voltage output of 0–360 mV which is amplified to a 0–3 V signal. The driving voltage was produced using an Agilent signal generator connected to a PDM200 amplifier module [20]. A second PDM200 module was used to generate the bias voltage. Using this set up, the 'Parallel', 'Biased Unipolar', and the new 'Biased Bipolar' electrical configurations were tested. The 'Bridged Bipolar' and 'Series' configurations were not tested as these configurations are electrically identical to the others tested.

Table 2 lists the static analytical and experimental results for the maximum tip deflection (δ_{max}), maximum blocking force (F_{blk}), relative deflection/force factor (γ) and the hysteresis. The measured deflection is the peak deflection achieved when driven with a 5 Hz sinusoidal waveform, which is also plotted in Fig. 8. The force was measured statically by applying a step input to the bender and measuring the DC change. The hysteresis was calculated from the maximum variation between rise and fall expressed as a percentage of the full span range. The deflection and hysteresis of the bender excited with a 1 Hz triangle wave is plotted in Fig. 9. The difference between the analytical results and the experimental results is attributed to imperfect geometry and tolerances in the d_{31} constant of the bender used.

In the experiment, the 'Biased Bipolar' configuration achieved a 37% increase in the tip deflection compared to the 'Biased

Table 2
Piezoelectric bender performance.

		Parallel	Unipolar	Bipolar
Experimental	Hysteresis (%)	16.06	18.21	19.31
	δ_{\max} (mm)	1.235	2.141	2.947
	F_{blk} (N)	0.382	0.629	0.826
	Relative δ	100%	173%	239%
	Effective Gain ($\mu\text{m/V}$)	13.7	14.3	15.1
Analytical	δ_{\max} (mm)	0.774	1.290	1.677
	F_{blk} (N)	0.195	0.325	0.423
	Relative δ	100%	167%	217%

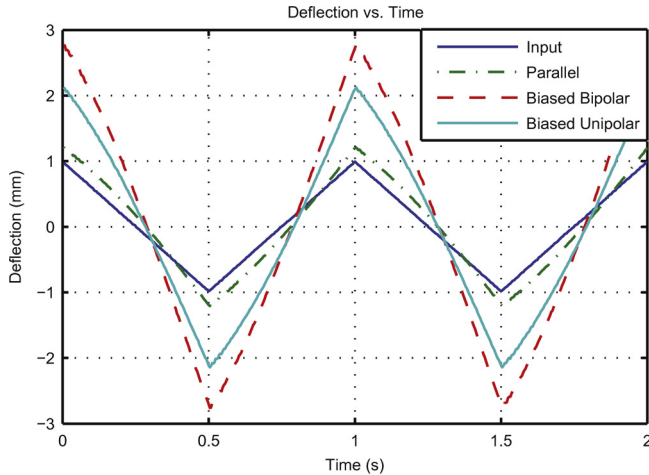


Fig. 9. Deflection and input vs time.

Unipolar' configuration. This increase is owed to the greater peak-to-peak voltage V_{pp} applied to each dielectric layer. The 'Biased Bipolar' configuration results in voltage range of 390 V compared to a 300 V for the 'Biased Unipolar' configuration. The difference is due to the application of both positive and negative voltages which utilizes the full range of the polling and coercive electric fields.

8. Conclusion

This paper describes a new electrical configuration for bimorph and multimorph piezoelectric benders. The new configuration operates by biasing the top electrode such that the full voltage range can be applied across all piezoelectric elements. An analytical analysis showed that the expected deflection is 117% greater than the parallel configuration and 30% greater than the biased unipolar arrangement. Experimental results demonstrate an improvement of 37% and 139% over the standard biased and parallel configurations respectively.

References

- [1] K. Uchino, J.R. Giniewica, *Micromechanics*, Marcel Dekker Inc., New York, 2003.
- [2] B. Potsaid, J.T. Wen, M. Unrath, D. Watt, M. Alpay, High performance motion tracking control for electronic manufacturing, *J. Dyn. Syst. Meas. Control* 129 (2007) 767–776.
- [3] S.S. Aphale, A.J. Fleming, S.O.R. Moheimani, Integral resonant control of collocated smart structures, *IOP Smart Mater. Struct.* 16 (2007) 439–446.
- [4] A.T. Baisch, P. Sreetharan, R.J. Wood, Biologically-inspired locomotion of a 2g hexapod robot, in: 2010 IEEE/RSJ International Conference on Intelligent Robots and Systems (IROS), IEEE, 2010, pp. 5360–5365.
- [5] Q.-M. Wang, L.E. Cross, Constitutive equations of symmetrical triple layer piezoelectric benders, *IEEE Trans. Ultrason. Ferroelectr. Freq. Control* 46 (6) (1999) 1343–1351.
- [6] C.B. Sawyer, The use of Rochelle salt crystals for electrical reproducers and microphones, *Proc. Inst. Radio Eng.* 19 (11) (1931) 2020–2029.
- [7] C.B. Sawyer, Piezoelectric device, US Patent RE20,213 (December 22, 1936).
- [8] S. Hayashi, T. Kittaka, A. Ando, Method of driving piezoelectric bimorph device and piezoelectric bimorph device, US Patent 5,233,256 (August 3, 1993).
- [9] R. Wood, E. Steltz, R. Fearing, Optimal energy density piezoelectric bending actuators, *Sens. Actuators A: Phys.* 119 (2) (2005) 476–488.
- [10] A. Morikawa, J. Inoue, J. Tabata, Piezoelectric bimorph type actuator, US Patent 5,382,864 (January 17, 1995).
- [11] D.J. Arbogast, F.T. Calkins, Electrical system for electrostrictive bimorph actuator, US Patent 6,888,291 (May 3, 2005).
- [12] J.G. Smits, S.I. Dalke, T.K. Cooney, The constituent equations of piezoelectric bimorphs, *Sens. Actuators A: Phys.* 28 (1) (1991) 41–61.
- [13] D. Campolo, R. Sahai, R.S. Fearing, Development of piezoelectric bending actuators with embedded piezoelectric sensors for micromechanical flapping mechanisms, in: IEEE International Conference on Robotics and Automation. Proceedings. ICRA'03, vol. 3, IEEE, 2003, pp. 3339–3346.
- [14] R. Sahai, S. Avadhanula, R. Groff, E. Steltz, R. Wood, R.S. Fearing, Towards a 3g crawling robot through the integration of microrobot technologies, in: Proceedings 2006 IEEE International Conference on Robotics and Automation. ICRA, IEEE, 2006, pp. 296–302.
- [15] F. Becker, K. Zimmermann, V.T. Minchenya, T. Volkova, Piezo-driven micro robots for different environments: prototypes and experiments, in: 7th German Conference on Robotics: Proceedings of ROBOTIK, VDE, 2012, pp. 1–5.
- [16] B.L. Siegal, Mounting for piezoelectric bender of fluid control device, US Patent 4,629,926 (December 16, 1986).
- [17] R. H.-J. Hohne, K. Mista, Warp knitting machine with piezoelectrically controlled bending transducers for the thread guides, US Patent 5,553,470 (September 10 1996).
- [18] J. McElroy, P. Thompson, H. Walker, E. Johnson, D. Radecki, R. Reynolds, Laser tuners using circular piezoelectric benders, *Appl. Opt.* 14 (6) (1975) 1297–1302.
- [19] Piezo System: Piezoceramic (September 2013). <http://www.piezo.com/index.html>
- [20] Piezodrive – high performance voltage and charge drive amplifiers for driving piezoelectric actuators (September 2013). <http://www.piezodrive.com/>
- [21] S.A. Rios, A.J. Fleming, A Novel Electrical Configuration for Three Wire Piezoelectric Bimorph, 2014.

Biographies

Shannon A. Rios graduated from The University of Newcastle, Australia (Callaghan campus) with a Bachelor of Electrical Engineering in 2012. His research areas include piezoelectric actuators, miniature robotics, gait control and miniature aerial vehicles. He is currently working toward a Ph.D. under the University of Newcastle Postgraduate Research scholarship.

Andrew J. Fleming graduated from The University of Newcastle, Australia (Callaghan campus) with a Bachelor of Electrical Engineering in 2000 and Ph.D. in 2004. Dr. Fleming is presently an Australian Research Council Future Fellow at the School of Electrical Engineering and Computer Science, The University of Newcastle, Australia. His research includes nanofabrication, micro-robotics, metrological sensing, nano-positioning, and high-speed scanning probe microscopy. Dr. Fleming's research awards include the IEEE Transactions on Control Systems Technology Outstanding Paper Award, The Australian Control Conference Best Student Paper Award, The University of Newcastle Researcher of the Year Award, and the Faculty of Engineering and Built Environment Award for Research Excellence. He is the co-author of three books and more than one-hundred Journal and Conference papers. Dr. Fleming is the inventor of several patent applications, in 2012 he received the Newcastle Innovation Rising Star Award for Excellence in Industrial Engagement.